

The impact of interfacial Si contamination on GaN-on-GaN regrowth for high power vertical devices

Cite as: Appl. Phys. Lett. **118**, 222104 (2021); <https://doi.org/10.1063/5.0049473>

Submitted: 05 March 2021 . Accepted: 21 May 2021 . Published Online: 02 June 2021

 Kai Fu,  Houqiang Fu, Xuguang Deng,  Po-Yi Su,  Hanxiao Liu, Kevin Hatch, Chi-Yin Cheng,  Daniel Messina, Reza Vatan Meidanshahi,  Prudhvi Peri,  Chen Yang, Tsung-Han Yang, Jossue Montes,  Jingan Zhou,  Xin Qi, Stephen M. Goodnick,  Fernando A. Ponce, David J. Smith,  Robert Nemanich, Yuji Zhao, et al.



View Online



Export Citation



CrossMark

ARTICLES YOU MAY BE INTERESTED IN

High-mobility n^- -GaN drift layer grown on Si substrates

Applied Physics Letters **118**, 222106 (2021); <https://doi.org/10.1063/5.0049133>

2DEGs formed in AlN/GaN HEMT structures with AlN grown at low temperature

Applied Physics Letters **118**, 222103 (2021); <https://doi.org/10.1063/5.0050584>

Non-polar true-lateral GaN power diodes on foreign substrates

Applied Physics Letters **118**, 212102 (2021); <https://doi.org/10.1063/5.0051552>

HIDEN
ANALYTICAL

Instruments for Advanced Science

- Knowledge,
- Experience,
- Expertise

[Click to view our product catalogue](#)

Contact Hiden Analytical for further details:

www.HidenAnalytical.com
info@hiden.co.uk



Gas Analysis

- ▶ dynamic measurement of reaction gas streams
- ▶ catalysis and thermal analysis
- ▶ molecular beam studies
- ▶ dissolved species probes
- ▶ fermentation, environmental and ecological studies



Surface Science

- ▶ UHVTPD
- ▶ SIMS
- ▶ end point detection in ion beam etch
- ▶ elemental imaging - surface mapping



Plasma Diagnostics

- ▶ plasma source characterization
- ▶ etch and deposition process reaction kinetic studies
- ▶ analysis of neutral and radical species



Vacuum Analysis

- ▶ partial pressure measurement and control of process gases
- ▶ reactive sputter process control
- ▶ vacuum diagnostics
- ▶ vacuum coating process monitoring

The impact of interfacial Si contamination on GaN-on-GaN regrowth for high power vertical devices

Cite as: Appl. Phys. Lett. **118**, 222104 (2021); doi: 10.1063/5.0049473

Submitted: 5 March 2021 · Accepted: 21 May 2021 ·

Published Online: 2 June 2021



View Online



Export Citation



CrossMark

Kai Fu,^{1,a)} Houqiang Fu,² Xuguang Deng,¹ Po-Yi Su,³ Hanxiao Liu,³ Kevin Hatch,³ Chi-Yin Cheng,¹ Daniel Messina,³ Reza Vatan Meidanshahi,¹ Prudhvi Peri,⁴ Chen Yang,¹ Tsung-Han Yang,¹ Jossue Montes,¹ Jingan Zhou,¹ Xin Qi,¹ Stephen M. Goodnick,¹ Fernando A. Ponce,³ David J. Smith,³ Robert Nemanich,³ and Yuji Zhao^{1,a)}

AFFILIATIONS

¹School of Electrical, Computer and Energy Engineering, Arizona State University, Tempe, Arizona 85287, USA

²Department of Electrical and Computer Engineering, Iowa State University, Ames, Iowa 50011, USA

³Department of Physics, Arizona State University, Tempe, Arizona 85287, USA

⁴School for Engineering of Matter, Transport and Energy, Arizona State University, Tempe, Arizona 85287, USA

^{a)}Authors to whom correspondence should be addressed: kaifu@asu.edu and yuji.zhao@asu.edu

ABSTRACT

The development of gallium nitride (GaN) power devices requires a reliable selective-area doping process, which is difficult to achieve because of ongoing challenges associated with the required etch-then-regrow process. The presence of silicon (Si) impurities of unclear physical origin at the GaN regrowth interface has proven to be a major bottleneck. This paper investigates the origin of Si contamination at the epitaxial GaN-on-GaN interface and demonstrates an approach that markedly reduces its impact on device performance. An optimized dry-etching approach combined with UV-ozone and chemical etching is shown to greatly reduce the Si concentration levels at the regrowth interface, and a significant improvement in a reverse leakage current in vertical GaN-based p-n diodes is achieved.

Published under an exclusive license by AIP Publishing. <https://doi.org/10.1063/5.0049473>

Gallium nitride (GaN) is a highly promising material candidate for applications in power electronics because of its superior physical and chemical properties. GaN power devices can offer significant improvements in energy conversion efficiency, switching frequency, and system volume over conventional silicon (Si) power devices.¹⁻³ To exploit the full potential of GaN and expand the device design space, selective-area doping is essential for GaN power devices, especially for vertical devices grown on bulk GaN substrates. However, mature doping methods such as ion implantation, diffusion of dopants, and epitaxy, which are commonly used in Si and gallium arsenide (GaAs) devices, are difficult to implement for GaN, especially for *p*-type doping. For the ion implantation approach, it was found that GaN was not very resistant to ion beam disordering, and this problem became more severe at higher doses.⁴ In the diffusion approach, the high dislocation density in GaN can strongly affect the effective diffusion penetration depth, and surface dissociation becomes significant during high-temperature annealing.⁵ The epitaxy (or regrowth) approach, i.e., doping through regrowth at selective

regions, is currently the most effective way to obtain well-controlled selective-area doping.

To achieve a selective-area doping by regrowth, dry etching is essential in forming the selective epitaxial regions. However, the etch-then-regrow process is very challenging and induces serious interface issues. First, the regrowth interface introduces high concentrations of impurities such as Si, carbon (C), and oxygen (O) even without any etching. These impurities may not be a problem for re-growing *n*-type GaN since Si and O are shallow donors for *n*-doping. However, these impurities are highly undesirable for the regrowth of *p*-GaN since they can compensate acceptors and reduce hole concentrations.⁶ Second, the dry etching process can introduce etching damage at the regrowth interface.⁷⁻⁹ Because of these problems, regrown *p-n* junctions have suffered from a high leakage current and a premature breakdown, which are two of the most serious challenges for selective-area regrowth and doping.

Different *ex situ* and *in situ* cleaning processes have been investigated since the 1980s to remove unwanted impurities and produce

atomically clean GaN surfaces.¹⁰ Wet chemical treatments, such as HCl:DI, NH₄OH:H₂O₂, diluted HF, NH₄F, BHF, H₂SO₄:H₂O₂, H₃PO₄, RCA SC1, and RCA SC2, are usually explored as *ex situ* methods.¹⁰ Dilute HF and HCl solutions were found to be the most effective in reducing C and O impurities, although large residual concentrations were also detected.¹⁰ Thermal desorption through annealing in metal-organic chemical vapor deposition (MOCVD) or molecular beam epitaxy (MBE) chambers is used for *in situ* cleaning. Annealing in NH₃ at 700–800 °C or multi-step alternating growth and annealing under vacuum at 780 °C could effectively remove C and O.^{10,11}

Despite the encouraging progress, the remaining important questions are how to remove the Si at the regrowth interface and where the Si comes from. Although very high concentrations of Si were commonly observed at regrowth interfaces,^{6,11,12} there were very few reports on the topic until the 2000s.^{12–14} For *ex situ* cleaning, UV-ozone exposure followed by HF dip has been found to remove almost 75% of the residual Si,¹⁴ which has been developed and applied to the fabrication of GaN MOSFETs with a regrown channel.^{15,16} The Si concentration can also be reduced by reducing the deposition temperature of a SiO₂ mask in selective-area growth for GaN MOSFETs due to the suppressed reaction between Si and GaN and the reduced bonding energy of SiO₂ at a lower temperature.¹⁷ For *in situ* cleaning, a C-doped layer can effectively compensate residual Si.^{11,14,18–21} Furthermore, both the *ex situ* and *in situ* methods are also helpful in reducing dry etching damage. Reducing etching power can also effectively reduce etching damage and leakage currents.^{7–9,22} However, the residual Si is still an intractable problem for regrowth, and its origins remain unclear.

In this work, we have comprehensively investigated the sources of Si impurities at the GaN regrowth interface. Different treatments were applied to GaN surfaces before regrowth, resulting in different Si concentrations at the interface. Based on these experimental results, a mechanism is proposed to explain the origin of Si impurities at the regrowth interface. The influence of Si impurities on the electrical performance of regrown *p-n* diodes is also studied, especially focusing on the etch-then-regrow process.

To investigate the effects of different treatments on impurities at the regrowth interface, a sample with multiple regrowth interfaces was homoepitaxially grown by metal-organic chemical vapor deposition (MOCVD) on a *c*-plane *n*⁺-GaN substrate with a carrier concentration of $\sim 10^{18}$ cm⁻³. The regrowth process is shown in Fig. 1(a). Five different treatment approaches were carried out before the GaN regrowth [Fig. 1(b)]: (1) apply organic cleaning (acetone/isopropanol/de-ionized water) to the GaN substrate, (2) remove the sample from the MOCVD chamber and leave it (in a plastic box) in the air for ~ 1 day, (3) leave the sample in the chamber at room temperature for 30 min, (4) etch the sample using inductively coupled plasma (ICP) etching (ICP power = 400 W, RF power = 70 W, pressure = 5 mTorr, Cl₂ = 30 sccm, and BCl₃ = 8 sccm) for 2 min and then treat the sample using UV-ozone and dilute HF and HCl (this treatment is referred to here as UV and chemicals), and (5) etch the sample using inductively coupled plasma (ICP) etching (ICP power = 400 W, RF power = 5 W, pressure = 5 mTorr, Cl₂ = 30 sccm, and BCl₃ = 8 sccm) for 2 min and treat the sample using UV-ozone and dilute HF and HCl. After each treatment step, 1 μ m of unintentionally doped (UID) GaN was then regrown on the surface. As shown in Fig. 1(b), these regrowth interfaces are denoted as “organic cleaning,” “leave in air for

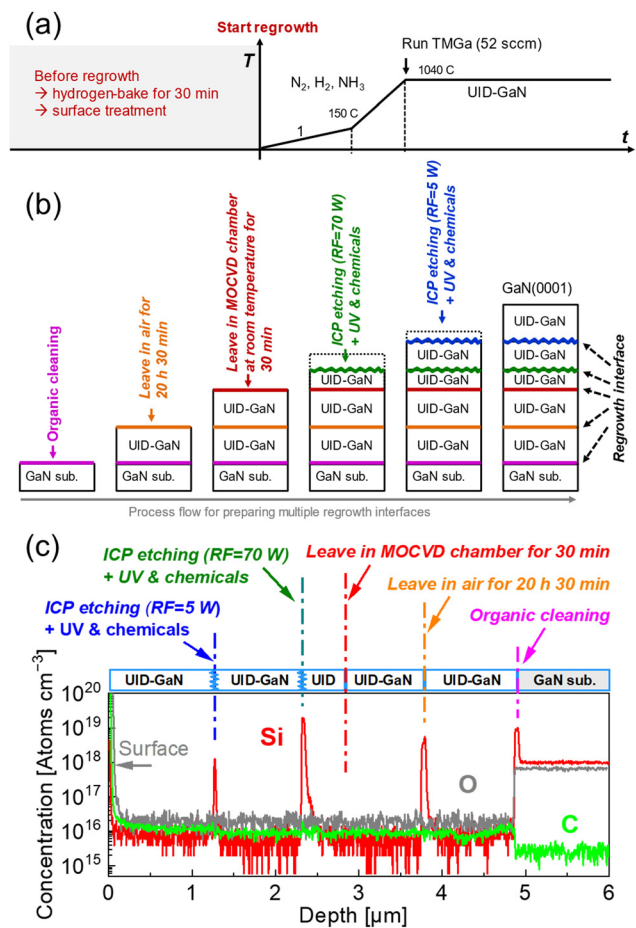


FIG. 1. (a) Schematic of a regrowth process by MOCVD. (b) Schematic of treatments to regrowth interfaces before regrowth. (c) SIMS profile of the samples with multiple regrowth interfaces.

20 h 30 min,” “leave in MOCVD chamber for 30 min,” “ICP etching (RF = 70 W) + UV and chemicals,” and “ICP etching (RF = 5 W) + UV and chemicals.”

Contaminants at the regrowth interfaces were analyzed by secondary ion mass spectrometry (SIMS), as shown in Fig. 1(c). No discernible peaks of C and O at the regrowth interfaces are observed for any treatment. However, there are very high concentrations of Si up to 10^{19} atoms cm⁻³ at several regrowth interfaces. Notable results include the following: (1) there were no Si impurities for the regrowth of “leave in MOCVD chamber for 30 min,” (2) high concentration of Si impurities appeared at the regrowth interfaces if the sample was removed from the MOCVD chamber into the air and reloaded into the chamber for regrowth, no matter whether it was etched or not, no matter what the etching power was, and no matter how the surface was treated, and (3) surface treatments before regrowth as well as ICP etching parameters affected the Si concentrations at the regrowth interfaces. According to the regrowth process, the Si impurities may come from: (1) a low impurity source that contains Si-related impurities,²³ (2) residual Si-related impurities in the MOCVD chamber that is

about $1 \times 10^{16} \text{ cm}^{-3}$ in this work, (3) surface preparation process, such as etching,^{24,25} and (4) Si compounds in the atmosphere, such as cyclic siloxanes,²⁶ which is at the level of $\sim 10^{10} \text{ cm}^{-3}$. Because there were no Si impurities for the regrowth of “leave in MOCVD chamber

for 30 min,” reasons (1) and (2) can be eliminated. Because Si impurities appeared for the regrowth of “leave in air for 20 h 30 min,” which did not contain an etching process or other Si-related tools, possible reason (3) can be ruled out. Thus, reason (4) seems to be the most

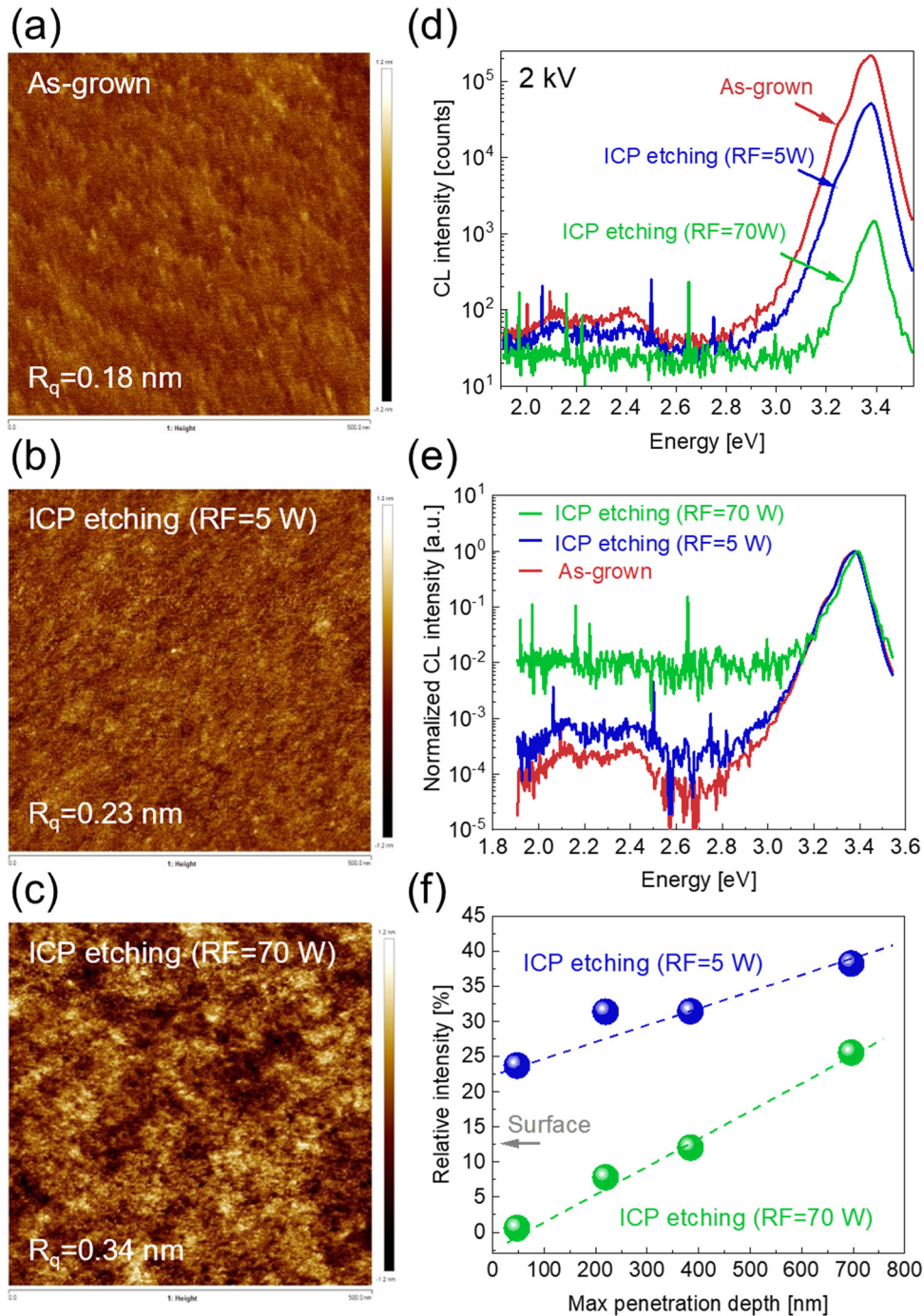


FIG. 2. Surface roughness of (a) as-grown sample, (b) ICP etching (RF = 5 W) sample, and (c) ICP etching (RF = 70 W) sample. (d) CL spectra of as-grown, ICP etching (RF = 5 W), and ICP etching (RF = 70 W) samples. (e) Normalized CL spectra of as-grown, ICP etching (RF = 5 W), and ICP etching (RF = 70 W) samples. (f) Relative CL intensity of ICP etching (RF = 5 W) and ICP etching (RF = 70 W) samples as a function of maximum electron penetration depth compared with the as-grown sample. Dashed lines show the linear fitting.

likely since it was also found that the Si impurities were able to be reduced if the sample was exposed to air for less time and that the amount of Si could be reduced by placing the sample in a N_2 box. However, for the regrowth of “ICP etching (RF = 70 W) + UV and chemicals” and “ICP etching (RF = 5 W) + UV and chemicals,” the sample was exposed to air for almost the same amount of time (about 10 min), but showed quite different Si concentrations. In addition, the amount of cyclic siloxanes in the air is at a very low level compared with the concentration of Si impurities at the regrowth interface. Hence, none of the possible reasons can directly explain the origin of the Si impurities, or there should be other factors that promote the adsorption of the Si.

According to x-ray photoelectron spectroscopy (XPS) measurements, the amount of surface band bending before regrowth of “leave in MOCVD chamber for 30 min,” “ICP etching (RF = 5 W) + UV and chemicals,” and “ICP etching (RF = 70 W) + UV and chemicals” was 0.7, 0.5, and 0.4 eV, respectively. The decrease in surface band bending compared with a clean GaN surface indicates an increase in positive surface states and/or ionized donors (positive).²⁷ Since the ionized donors should be the same for all samples, the decrease in surface band bending must mainly be due to an increase in positive surface states that cause more Si incorporation at the interface during the regrowth. In addition to the fact that higher RF power led to more Si, it is also well known that dry etching could cause nitrogen vacancies and/or gallium dangling bonds, which can be the source for positive charge states.^{27–30} Moreover, oxidation is almost inevitable before the growth, and a longer oxidation time tends to cause higher Si contaminants after regrowth, suggesting that oxygen atoms can act as the intermediate medium to increase the Si adsorption during regrowth. Therefore, we deduce that: (1) residual Si-related impurities in the MOCVD chamber are the main source for Si impurities, but only with the help of a specific surface state can a high concentration of Si impurities be formed on the GaN surface, (2) higher concentration of nitrogen vacancies and/or gallium dangling bonds at the surface, such as caused by etching, could enhance the Si adsorption, (3) oxidation is another process that can enhance the Si adsorption, and (4) Si compounds present in the atmosphere, such as cyclic siloxane, could be another source for the Si impurities but have a very limited contribution.

According to this discussion, one way to reduce the Si impurities at the regrowth interface is to reduce the surface nitrogen vacancies and/or gallium dangling bonds, or else reduce the etching damage. The atomic force microscope (AFM) analysis in Figs. 2(a)–2(c) shows that lower RF power can effectively reduce the surface roughness and lead to a smoother regrowth surface. The surface damage was also studied by cathodoluminescence (CL). The intensity of band edge emissions decreased with RF powers, indicating that more damage was induced when applying a higher RF power [Fig. 2(d)]. Normalized CL spectrum shows ICP etching has little effect on the spectral shape of band edge emission [Fig. 2(e)]. However, the relative intensity of the yellow luminescence increased with the RF power, suggesting an enhancement of electron capture from conduction bands or shallow donors by deep acceptors.³¹ This is consistent with the increase in nitrogen vacancies due to dry etching since a nitrogen-vacancy behaves as a shallow compensating center.^{28–30} Figure 2(f) shows relative luminescence intensities of the etched samples normalized to the as-grown sample as a function of electron penetration

depth. The relative intensity increased with the electron penetration depth or at lower RF power, indicating that more severe etching damage is closer to the surface and caused by higher RF power.

To investigate the impact of the Si impurities on the electrical performance of GaN devices, different treatments were applied to the surfaces of 9 μm -thick UID-GaN homoepitaxially grown by MOCVD on *c*-plane n^+ -GaN (0001) substrates, followed by the regrowth of a UID-GaN insertion layer and 500 nm-thick *p*-GaN, as shown in Fig. 3(a). Several conclusions can be made by comparing the device leakage and the relationship between leakage and Si concentration at the regrowth interface [Fig. 3(b)]. First, devices with Si concentrations higher than $1 \times 10^{19} \text{ cm}^{-3}$ show very similar high leakage current. Second, the leakage current increases markedly as the Si concentration at the regrowth interface increases. Third, ICP etching with low RF power combining with UV and chemicals is very effective in reducing the reverse leakage current.

In addition to reverse leakage current, the ideality factor is another important factor for *p*-*n* diodes. When the recombination of carriers in the space charge region dominates, the ideal factor will be close to 2.³² When the diffusion current dominates, it will be close to 1.³² Ideality factors higher than 2 are usually attributed to trap-assisted tunneling.^{33–36} Regrown GaN *p*-*n* diodes usually have very large ideality factors,^{6,9} which are caused by enhanced tunneling at the regrowth interface, resulting from the coexistence of high concentrations of Mg and Si.³⁷ By comparing the forward performance as shown in Fig. 4, three important insights can be obtained for regrown GaN *p*-*n* junctions. First, cleaning using UV and chemicals is very effective in reducing the ideality factor compared with organic cleaning. Second, a thicker insertion layer is helpful to reduce the ideality factor since it moves the peak electric field in the *p*-*n* junction far away from the

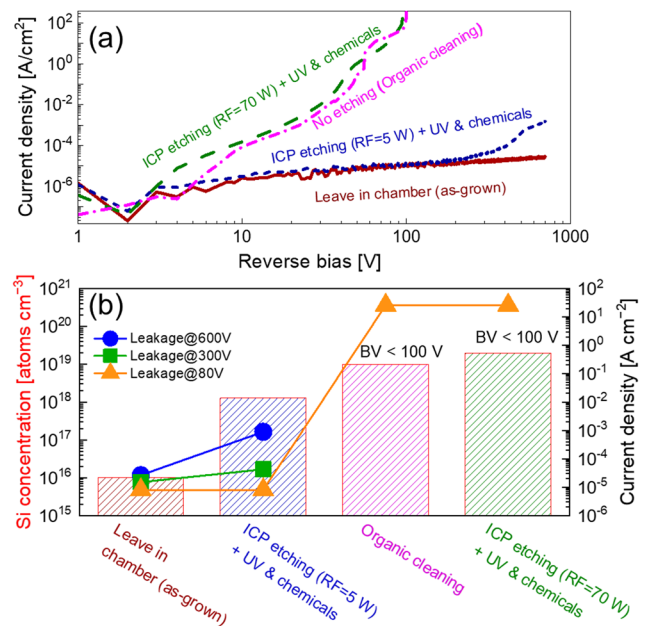


FIG. 3. (a) Reverse leakage of the *p*-*n* diodes by different treatments to regrowth interfaces. (b) Comparison between the leakage current (dots) and Si concentration at the regrowth interface (histogram).

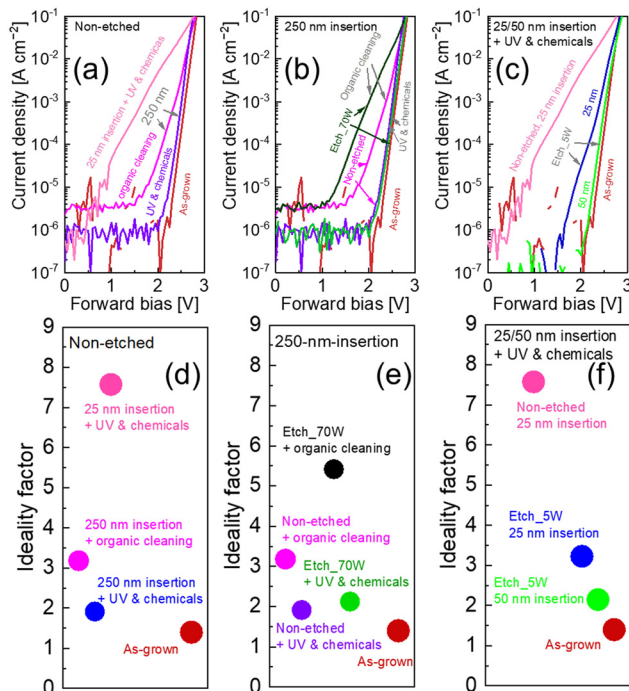


FIG. 4. Forward curves of (a) non-etched samples, (b) samples with 250 nm-thick insertion, and (c) samples with 25 nm- or 50 nm-thick insertion including treatment of UV and chemicals. Ideality factors of (d) non-etched samples, (e) samples with 250 nm-thick insertion, and (f) samples with 25 nm- or 50 nm-thick insertion including treatment of UV and chemicals.

interface with high-density trap levels, thereby reducing the tunneling current. Third, appropriate etching conditions are even more conducive in terms of reducing ideality factors than non-etching.

In summary, the origin of Si impurities at the regrowth interface of the *c*-plane GaN has been investigated. It was found that (1) residual Si-related impurities in the MOCVD chamber are the main source for Si impurities, but only with the help of a specific surface state can a high concentration of Si impurities be formed on the GaN surface and (2) nitrogen vacancies and/or gallium dangling bonds at the surface and/or oxidation could enhance the Si adsorption. A high concentration of Si impurities at the regrowth interface could result in an enhanced local electric field, reduced space charge region, high reverse leakage current, and large ideality factor. Overall, it was found that suitable ICP etching combined with treatment with UV and chemicals can greatly reduce the reverse leakage current and ideality factor of the regrown GaN p-n diodes.

AUTHORS' CONTRIBUTIONS

K.F., H.F., and X.D. contributed equally to this work.

This work was supported in part by ARPA-E PNDIODES Program under Grant No. DE-AR0000868, in part by the NASA HOTTech Program under Grant No. 80NSSC17K0768, in part by the ASU Nanofab through NSF under Contract No. ECCS-1542160, and in part by ULTRA, an Energy Frontier Research

Center funded by the U.S. Department of Energy, Office of Science, BaEsic Energy Sciences under Award No. DE-SC0021230.

DATA AVAILABILITY

The data that support the findings of this study are available from the corresponding author upon reasonable request.

REFERENCES

- U. K. Mishra, L. Shen, T. E. Kazior, and Y. Wu, *Proc. IEEE* **96**, 287 (2008).
- B. J. Baliga, *Semicond. Sci. Tech.* **28**, 074011 (2013).
- E. A. Jones, F. F. Wang, and D. Costinett, *IEEE J. Emerging Sel. Top. Powers* **4**, 707 (2016).
- S. Kucheyev, J. Williams, and S. Pearton, *Mater. Sci. Eng., R* **33**, 51 (2001).
- J. K. Sheu and G. C. Chi, *J. Phys.: Condens. Matter* **14**, R657 (2002).
- K. Fu, H. Fu, H. Liu, S. R. Alugubelli, T.-H. Yang, X. Huang, H. Chen, I. Baranowski, J. Montes, F. A. Ponce, and Y. Zhao, *Appl. Phys. Lett.* **113**, 233502 (2018).
- D. G. Kent, K. P. Lee, A. P. Zhang, B. Luo, M. E. Overberg, C. R. Abernathy, F. Ren, K. D. Mackenzie, S. J. Pearton, and Y. Nakagawa, *Solid-State Electron.* **45**, 1837 (2001).
- T. Narita, D. Kikuta, N. Takahashi, K. Kataoka, Y. Kimoto, T. Uesugi, T. Kachi, and M. Sugimoto, *Phys. Status Solidi A* **208**, 1541 (2011).
- K. Fu, H. Fu, X. Huang, H. Chen, T. Yang, J. Montes, C. Yang, J. Zhou, and Y. Zhao, *IEEE Electron Device Lett.* **40**, 1728 (2019).
- S. W. King, J. P. Barnak, M. D. Bremser, K. M. Tracy, C. Ronning, R. F. Davis, and R. J. Nemanich, *J. Appl. Phys.* **84**, 5248 (1998).
- G. Koblmüller, R. M. Chu, A. Raman, U. K. Mishra, and J. S. Speck, *J. Appl. Phys.* **107**, 043527 (2010).
- H. Xing, S. P. DenBaars, and U. K. Mishra, *J. Appl. Phys.* **97**, 113703 (2005).
- H. Xing, D. S. Green, H. Yu, T. Mates, P. Kozodoy, S. Keller, S. P. DenBaars, and U. K. Mishra, *Jpn. J. Appl. Phys., Part 1* **42**, 50 (2003).
- S. Chowdhury, Ph.D. thesis (University of California, Santa Barbara, 2010).
- D. Ji, C. Gupta, S. H. Chan, A. Agarwal, W. Li, S. Keller, U. K. Mishra, and S. Chowdhury, in *IEEE International Electron Devices Meeting (IEDM)* (IEEE, 2017), p. 9.4.1.
- W. Li, K. Nomoto, K. Lee, S. M. Islam, Z. Hu, M. Zhu, X. Gao, M. Pilla, D. Jena, and H. G. Xing, *IEEE Trans. Electron. Devices* **65**, 2558 (2018).
- F. Yang, Y. Yao, Z. He, G. Zhou, Y. Zheng, L. He, J. Zhang, Y. Ni, D. Zhou, Z. Shen, J. Zhong, Z. Wu, B. Zhang, and Y. Liu, *J. Mater. Sci.* **26**, 9753 (2015).
- D. S. Green, U. K. Mishra, and J. S. Speck, *J. Appl. Phys.* **95**, 8456 (2004).
- C. Poblentz, P. Waltereit, S. Rajan, S. Heikman, U. K. Mishra, and J. S. Speck, *J. Vac. Sci. Technol. B* **22**, 1145 (2004).
- D. F. Storm, D. S. Katzer, S. C. Binari, B. V. Shanabrook, X. Xu, D. S. McVey, R. P. Vaudo, and G. R. Brandes, *Electron. Lett.* **40**, 1226 (2004).
- S. Haffouz, H. Tang, S. Rolfé, and J. A. Bardwell, *Appl. Phys. Lett.* **88**, 252114 (2006).
- M. Kato, K. Mikamo, M. Ichimura, M. Kanetchika, O. Ishiguro, and T. Kachi, *J. Appl. Phys.* **103**, 093701 (2008).
- M. J. Manfra, N. G. Weimann, J. W. P. Hsu, L. N. Pfeiffer, K. W. West, S. Syed, H. L. Stormer, W. Pan, D. V. Lang, S. N. G. Chu, G. Kowach, A. M. Sergent, J. Caissie, K. M. Molvar, L. J. Mahoney, and R. J. Molnar, *J. Appl. Phys.* **92**, 338 (2002).
- W. Lee, J. H. Ryou, D. Yoo, J. Limb, R. D. Dupuis, D. Hanser, E. Preble, N. M. Williams, and K. Evans, *Appl. Phys. Lett.* **90**, 093509 (2007).
- J. P. Liu, J. H. Ryou, D. Yoo, Y. Zhang, J. Limb, C. A. Horne, S. C. Shen, R. D. Dupuis, A. D. Hanser, E. A. Preble, and K. R. Evans, *Appl. Phys. Lett.* **92**, 133513 (2008).
- R. A. Yucuis, C. O. Stanier, and K. C. Hornbuckle, *Chemosphere* **92**, 905 (2013).
- B. S. Eller, J. Yang, and R. J. Nemanich, *J. Electron. Mater.* **43**, 4560 (2014).
- K. Laaksonen, M. G. Ganchenkova, and R. M. Nieminen, *J. Phys.: Condens. Matter* **21**, 015803 (2009).
- Q. Yan, A. Janotti, M. Scheffler, and C. G. Van de Walle, *Appl. Phys. Lett.* **100**, 142110 (2012).

- ³⁰J. Buckeridge, C. R. A. Catlow, D. O. Scanlon, T. W. Keal, P. Sherwood, M. Miskufova, A. Walsh, S. M. Woodley, and A. A. Sokol, *Phys. Rev. Lett.* **114**, 016405 (2015).
- ³¹I. Shalish, L. Kronik, G. Segal, Y. Rosenwaks, Y. Shapira, U. Tisch, and J. Salzman, *Phys. Rev. B* **59**, 9748 (1999).
- ³²C. Sah, R. N. Noyce, and W. Shockley, *Proc. IRE* **45**, 1228 (1957).
- ³³H. C. Casey, J. Muth, S. Krishnakutty, and J. M. Zavada, *Appl. Phys. Lett.* **68**, 2867 (1996).
- ³⁴P. Perlin, M. Osinski, P. G. Eliseev, V. A. Smagley, J. Mu, M. Banas, and P. Sartori, *Appl. Phys. Lett.* **69**, 1680 (1996).
- ³⁵J. M. Shah, Y. L. Li, T. Gessmann, and E. F. Schubert, *J. Appl. Phys.* **94**, 2627 (2003).
- ³⁶D. Zhu, J. Xu, A. N. Noemaun, J. K. Kim, E. F. Schubert, M. H. Crawford, and D. D. Koleske, *Appl. Phys. Lett.* **94**, 081113 (2009).
- ³⁷S. R. Alugubelli, H. Fu, K. Fu, H. Liu, Y. Zhao, M. R. McCartney, and F. A. Ponce, *Appl. Phys. Lett.* **115**, 201602 (2019).